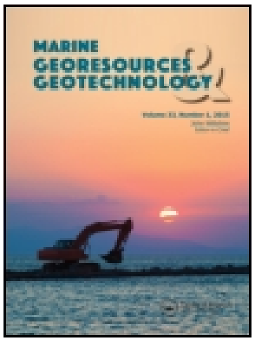

Taylor & Francis
Taylor & Francis Group

Marine Georesources & Geotechnology

ISSN: 1064-119X (Print) 1521-0618 (Online) Journal homepage: http://www.tandfonline.com/loi/umgt20

Vertical Dynamic Impedance of Large-Diameter Pile Considering Its Transverse Inertia Effect and Construction Disturbance Effect

Zhen-ya Li & Kui-hua Wang

To cite this article: Zhen-ya Li & Kui-hua Wang (2016): Vertical Dynamic Impedance of Large-Diameter Pile Considering Its Transverse Inertia Effect and Construction Disturbance Effect, Marine Georesources & Geotechnology, DOI: 10.1080/1064119X.2016.1149259

To link to this article: http://dx.doi.org/10.1080/1064119X.2016.1149259

Accepted author version posted online: 18 Feb 2016.

Vertical Dynamic Impedance of Large-diameter Pile Considering Its Transverse Inertia Effect and Construction Disturbance Effect

Zhen-ya Li

MOE Key Laboratory of Soft Soils and Geoenvironmental Engineering, Zhejiang University, Hangzhou, China

Research center of Coastal Urban Geotechnical Engineering, Zhejiang University, Hangzhou, China

Kui-hua Wang

MOE Key Laboratory of Soft Soils and Geoenvironmental Engineering, Zhejiang University, Hangzhou, China

Research center of Coastal Urban Geotechnical Engineering, Zhejiang University, Hangzhou, China

Address correspondence to

Abstract

The vertical dynamic impedance of the large-diameter pile is theoretically investigated considering the construction disturbance effect. First, the Rayleigh-Love rode model is introduced to simulate the large-diameter pile with the consideration of its transverse inertia effect. The shear complex stiffness transfer model is proposed to simulate the radial inhomogeneity of the pile surrounding soil caused by the construction disturbance effect. Then, the pile-soil system is divided into finite segments, and the governing equation of the pile-soil system subjected to vertical dynamic loading is established. Following this, the analytical solution of vertical dynamic impedance at the pile head is obtained by means of the shear complex stiffness transfer method and the impedance function transfer method. Based on the present solution, a parametric analysis is conducted to investigate the influence of the transverse inertia effect on the vertical dynamic impedance at the pile head and its relationship with the

pile-soil parameters. Finally, comparisons with published solutions are carried out to verify the reliability of the present solution.

Keywords: construction disturbance effect, impedance, large-diameter pile, shear complex stiffness, transverse inertia effect

INTRODUCTION

With the economic and social development, rapid industrialization and urbanization in the coastal areas have witnessed the implementation of a significant number of infrastructure constructions, such as high-rise buildings, bridges, ports, and so on. Besides, in order to solve the problems of energy shortage and environmental pollution, offshore wind farms are at the threshold of large-scale development. In these areas, the marine soft clay is noted as thick layer, high compressibility and low intensity, making the geological condition very complicated and the engineering very difficult. Because of its high bearing capacity, large stiffness and small settlement, large-diameter pile has been found broad application in these areas. Many investigators have studied the bearing capacity and settlement behaviors of large-diameter pile by utilizing theoretical research (Gao, Yang, et al. 2012; Gao, Gao, et al. 2012), filed tests and model tests (Zhu et al. 2012; Liu et al. 2013; Zhao et al. 2015). However, the research on the dynamic characteristic of large-diameter pile is insufficient.

In practice vertical dynamic loading often occurs in large-diameter pile foundations. As a result, it is of great importance to investigate the vertical dynamic response of large-diameter pile for the purpose of dynamic foundation design, earthquake-resistance design and dynamic pile testing. There are two main factors that make the dynamic response of large-diameter pile different from that of the slender bar.

The first is the size effect. The existing dynamic analysis models of pile mainly developed on the basis of one-dimensional (1D) wave theory (Novak 1974; Han and Sabin 1995; Wu et al. 2013) is not applicable to the large-diameter pile whose length-diameter ratio is usually less than 10 and the three-dimensional (3D) effect of wave propagation is obvious consequently, resulting in a significant difference between the field test result and the 1D solution (Li and Gong 1998; Chow et al. 2003; Chai, Phoon, and Zhang 2010; Chai et al. 2011) because of the wave dispersion effect. In order to deal with this problem, the Rayleigh-Love rod model was presented, in which the transverse inertia effect is deemed as a reflection of the 3D wave effect. Li, Wang, and Xie (2005) and Yang and Tang (2013) analyzed the longitudinal vibration of a large-diameter rock-socked pile embedded in homogeneous saturated soil by means of Rayleigh-Love rod model. Yu, Cai, and Wu (2013) investigated the influence of sediment on the vertical dynamic impedance in the low frequency range of the pile by considering the transverse inertia effect. Lü et al. (2014) and Wu, Wang, and Dou (2013) also used this model to analyze the dynamic response of pile.

The second is the construction disturbance effect. The soil surrounding the pile shaft may be weakened or strengthened according to the method of installation of pile, which results in a radially inhomogeneous soil layer. On the one hand, it may affect the bearing capacity of pile. Pells, Rowe, and Turner (1980) pointed out that the calculation coefficient of pile shaft resistance decreases with the increase of pile radius. Filed tests conducted by Liu et al. (2010) and Gong et al. (2012) indicated that the shaft resistance of large-diameter bored pile decreases because of the soil unloading during or after the hole-forming. The model test (He et al. 2015) and numerical analysis (Zhang, Wu, and Zhang 2007) showed the similar conclusion. Conversely, the bearing capacity of the large-diameter pile increases significantly due to the compaction effect of the surrounding soil (Kodikara and Moore 1993; El Naggar and Wei 2000). On the other hand, the radial inhomogeneity of soil has an important influence on the dynamic behavior of pile. Many scholars have paid their attention on this problem and contributed in some manner to the development of the pile vibration theory. Novak and Sheta (1980) proposed a weakened annular boundary zone around the foundation to simulate the weakening effect of the soil, in which the mass of the weakened boundary zone was assumed to be zero, thus neglecting its inertia effect. This limitation was soon overcome by Veletsos and Dotson (Veletos and Dotson 1986, 1988), but a homogeneous boundary zone with a nonzero mass may lead to highly undulatory varations in the frequency of the layer impedances due to wave reflections at the interface between two distinctly discontinuous zones (Novak and Han 1988). El Naggar (2000) further presented a discrete boundary zone model to investigate the dynamic impedance of the composite soil. In this model, the pile surrounding soil is assumed as a linear viscoelastic medium composed of two concentric regions, namely an inner zone that is further subdivided into many concentric annular soil subzones and an outer zone that is treated as undisturbed and homogeneous. However, this model does not treat the interaction of soil zones rigorously, which may lead to the question whether the results adequately reflect the real interaction of the soil zones (Yang et al. 2009).

It can be seen that great effort has been devoted to the influence of radially inhomogeneity of soil on the dynamic response of slender pile, but the research on that of the large-diameter pile is still insufficient. In light of this, in order to extend the application of large-diameter pile and provide the theoretical basis for dynamic design and earthquake-resistance design, the dynamic impedance of large-diameter pile embedded in radially inhomogeneous soil is investigated in this paper. The shear complex stiffness transfer model and Rayleigh-Love rod model are proposed to allow for the radial inhomogeneity of soil and the transverse inertia effect of pile, respectively. A parametric study is undertaken based on the solution to investigate the influence of the transverse inertia effect and the construction disturbance effect on the dynamic impedance of large-diameter pile.

MATHEMATICAL MODEL OF PILE-SOIL SYSTEM

The problem studied herein is the vertical vibration characteristics of a large-diameter pile considering the construction disturbance effect. The mathematical model of pile-soil system is shown in **Figure 1**, where l_{p} and $q(t)$ represent the pile length and the harmonic force acting on the pile head, respectively. By taking the layered characteristic of pile surrounding soil into account, the pile-soil system is discretized into a total of *n* segments from pile tip to pile head. The thickness and the depth of the upper interface of the *i*th pile-soil segment measured from the ground surface are denoted by l_i and h_i, respectively. The properties of pile are assumed to be homogeneous within each segment, but may vary from segment to segment.

Because of the construction disturbance, pile surrounding soil may be relaxed or compacted. The shear complex stiffness transfer model is proposed to deal with the inhomogeneity of pile surrounding soil in the radial direction. As shown in **Figure 1**, the pile surrounding soil is divided into *m* vertical annular zones numbered 1, 2, …, *j*, …, *m* in the radial direction and the outer radius of the *j*th zone within the *i*th soil layer is denoted by $r_{i,j}$. Soil reaction acting on the pile tip is simulated by means of single Voigt model, where k_{b} and δ_{b} represent the spring constant and the viscosity coefficient, respectively. According to Randolph and Deeks (Randolph and Deeks 1992), $k_{\mathrm{b}} = 8G_{\mathrm{b}} / \pi(1-\mu_{\mathrm{b}})d_{\mathrm{p}}, \delta_{\mathrm{b}} = 3.2G_{\mathrm{b}} / \pi(1-\mu_{\mathrm{b}})v_{\mathrm{b}}$, where $\mu_{\mathrm{b}}, v_{\mathrm{b}}, G_{\mathrm{b}} = \rho_{\mathrm{b}} v_{\mathrm{b}}^2$ and ρ_{b} represent the dynamic Poisson ratio, shear wave velocity, shear modulus and mass density of the pile end soil, respectively, d_{p} is the diameter of the pile.

The following assumptions are adopted during the investigation:

(1) The pile is a viscoelastic Rayleigh-Love rod with a uniform circular cross-section, and rests on viscoelastic support.

(2) The surrounding soil extends infinitely in the radial direction, and there are no normal or shear stresses on the free surface of the soil.

(3) The pile-soil system is subjected to small deformations and strains during the vibration, and the pile has a perfect contact with the soil.

(4) The dynamic stress of soil transfers to the pile shaft through the complex stiffness on the contact interface of pile-soil system.

GOVERNING EQUATIONS AND SOLUTIONS

Governing Equations

According to the plane stain model by Novak, Aboul-Ella, and Nogami (1978), the dynamic equation of the pile surrounding soil can be given as

$$r^2 \frac{\mathrm{d}^2 W_{i,j}(r)}{\mathrm{d}r^2} + r\frac{\mathrm{d}W_{i,j}(r)}{\mathrm{d}r} - s_{i,j}^2 r^2 W_{i,j}(r) = 0 \quad (1)$$

where $W_{i,j}(r)$ is the vertical displacement of the jth zone within the ith soil layer; $s_{i,j} = \xi / v_{\mathrm{s}i,j}\sqrt{1+\mathrm{j}\beta_{\mathrm{s}i,j}}$, $\xi = \mathrm{j}\omega$, $v_{\mathrm{s}i,j}$ and $\beta_{\mathrm{s}i,j}$ denote the shear wave velocity and material damping coefficient of soil, respectively, ω is the circular frequency and $\mathrm{j} = \sqrt{-1}$ is the imaginary unit.

To account for the transverse inertia effect of the large-diameter pile by the Rayleigh-Love rod model, the dynamic vibration equation of the ith pile segment can be written as

$$E_{\mathrm{p}i}A_{\mathrm{p}i}\frac{\partial^2 u_{\mathrm{p}i}(z,t)}{\partial z^2} + A_{\mathrm{p}i}\delta_{\mathrm{p}i}\frac{\partial^3 u_{\mathrm{p}i}(z,t)}{\partial z^2 \partial t} - \rho_{\mathrm{p}i}A_{\mathrm{p}i}\left[\frac{\partial^2 u_{\mathrm{p}i}(z,t)}{\partial t^2} - \mu_{\mathrm{p}i}^2 r_{\mathrm{p}i}^2 \frac{\partial^4 u_{\mathrm{p}i}(z,t)}{\partial z^2 \partial t^2}\right] - f_i(z,t) = 0 \quad (2)$$

where $u_{\mathrm{p}i}(z,t)$, $E_{\mathrm{p}i} = \rho_{\mathrm{p}i}v_{\mathrm{p}i}^2$, $A_{\mathrm{p}i} = \pi r_{\mathrm{p}i}^2$, $\rho_{\mathrm{p}i}$, $r_{\mathrm{p}i}$, $\delta_{\mathrm{p}i}$ and $\mu_{\mathrm{p}i}$ denote the vertical displacement, elastic modulus, sectional area, density, radius, material damping and dynamic Poisson ratio of the ith pile segment, respectively; $f_i(z,t)$ is the frictional force of the soil acting on the pile shaft, which can be obtained by $f_i(z,t) = K_{i,1}u_{\mathrm{p}i}(z,t)$, where $K_{i,1}$ is the shear complex stiffness of the pile-soil interface.

Boundary conditions at the pile head and pile tip:

$$\left[E_{\mathrm{p}n}A_{\mathrm{p}n}\frac{\partial u_{\mathrm{p}n}}{\partial z} + A_{\mathrm{p}n}\delta_{\mathrm{p}n}\frac{\partial^2 u_{\mathrm{p}n}}{\partial z \partial t} + \rho_{\mathrm{p}n}A_{\mathrm{p}n}\mu_{\mathrm{p}n}^2 r_{\mathrm{p}n}^2 \frac{\partial^3 u_{\mathrm{p}n}}{\partial z \partial t^2}\right]\Bigg|_{z=0} + q(t) = 0 \quad (3)$$

$$\left[(k_{\mathrm{b}}+\delta_{\mathrm{b}}\frac{\partial}{\partial t})u_{\mathrm{p}1}+(E_{\mathrm{p}1}+\delta_{\mathrm{p}1}\frac{\partial}{\partial t})\frac{\partial u_{\mathrm{p}1}}{\partial z}+\rho_{\mathrm{p}1}A_{\mathrm{p}1}\mu_{\mathrm{p}1}^{2}r_{\mathrm{p}1}^{2}\frac{\partial^{3}u_{\mathrm{p}1}}{\partial z\partial t^{2}}\right]\Bigg|_{z=l_{\mathrm{p}}}=0 \quad (4)$$

Boundary conditions at the interface of pile segment:

$$u_{\mathrm{p}i}(z,t)\big|_{z=h_i}=u_{\mathrm{p}i+1}(z,t)\big|_{z=h_i} \quad (5)$$

$$\begin{aligned}&\left[E_{\mathrm{p}i}A_{\mathrm{p}i}\frac{\partial u_{\mathrm{p}i}(z,t)}{\partial z}+A_{\mathrm{p}i}\delta_{\mathrm{p}i}\frac{\partial^{2}u_{\mathrm{p}i}(z,t)}{\partial z\partial t}+\rho_{\mathrm{p}i}A_{\mathrm{p}i}\mu_{\mathrm{p}i}^{2}r_{\mathrm{p}i}^{2}\frac{\partial^{3}u_{\mathrm{p}i}(z,t)}{\partial z\partial t^{2}}\right]\Bigg|_{z=h_i}\\&=\left[E_{\mathrm{p}i+1}A_{\mathrm{p}i+1}\frac{\partial u_{\mathrm{p}i+1}(z,t)}{\partial z}+A_{\mathrm{p}i+1}\delta_{\mathrm{p}i+1}\frac{\partial^{2}u_{\mathrm{p}i+1}(z,t)}{\partial z\partial t}+\rho_{\mathrm{p}i+1}A_{\mathrm{p}i+1}\mu_{\mathrm{p}i+1}^{2}r_{\mathrm{p}i+1}^{2}\frac{\partial^{3}u_{\mathrm{p}i+1}(z,t)}{\partial z\partial t^{2}}\right]\Bigg|_{z=h_i}\end{aligned} \quad (6)$$

Initial conditions of pile:

$$u_{\mathrm{p}i}(z,t)\big|_{t=0}=0 \quad (7)$$

$$\frac{\partial u_{\mathrm{p}i}(z,t)}{\partial t}\bigg|_{t=0}=0 \quad (8)$$

Solution of the Soil Layers' Vibration

Based on the partial differential theory, the equation of the soil is solved. Substituting the boundary condition that the stresses and displacements tend to be zero at an infinite radial distance into Eq. (1) and solving it gives

$$W_{i,j}(r)=\begin{cases}C_{i,j}\mathrm{K}_0(s_{i,j}r) & j=m\\ C_{i,j}\mathrm{K}_0(s_{i,j}r)+D_{i,j}\mathrm{I}_0(s_{i,j}r) & j=1,2,\ldots,m-1\end{cases} \quad (9)$$

where $\mathrm{I}_0(s_{i,j}r)$ and $\mathrm{K}_0(s_{i,j}r)$ are the modified Bessel functions of zero order of the first and second kinds, respectively; $C_{i,j}$ and $D_{i,j}$ are constants determined by the boundary conditions.

The soil shear stress of interface between the *j*th and (*j*-1)th zones can be obtained as

$$\tau_{i,j}(r_{i,j})=\begin{cases}-G_{i,j}^{*}s_{i,j}C_{i,j}\mathrm{K}_1(s_{i,j}r_{i,j}) & j=m\\ -G_{i,j}^{*}s_{i,j}\left[C_{i,j}\mathrm{K}_1(s_{i,j}r_{i,j})\text{-}D_{i,j}\mathrm{I}_1(s_{i,j}r_{i,j})\right] & j=1,2,\ldots,m-1\end{cases} \quad (10)$$

where $G_{i,j}^{*} = G_{i,j}\left(1+\mathrm{j}\,\beta_{\mathrm{s}i,j}\right)$, $G_{i,j} = \rho_{\mathrm{s}i,j} v_{\mathrm{s}i,j}^{2}$ and $\rho_{\mathrm{s}i,j}$ are the shear modulus and mass density of the *j*th soil zone within the *i*th soil layer, respectively.

The shear complex stiffness at the inner boundary of the *j*th zone within the *i*th soil layer can be given as:

$$K_{i,j} = \begin{cases} 2\pi r_{i,j} G_{i,j}^{*} s_{i,j} \mathrm{K}_1\left(s_{i,j} r_{i,j}\right) / \mathrm{K}_0\left(s_{i,j} r_{i,j}\right) & j = m \\ \dfrac{2\pi r_{i,j} G_{i,j}^{*} s_{i,j}\left[\dfrac{C_{i,j}}{D_{i,j}} \mathrm{K}_1\left(s_{i,j} r_{i,j}\right) \text{-} \mathrm{I}_1\left(s_{i,j} r_{i,j}\right)\right]}{\dfrac{C_{i,j}}{D_{i,j}} \mathrm{K}_0\left(s_{i,j} r_{i,j}\right) + \mathrm{I}_0\left(s_{i,j} r_{i,j}\right)} & j = 1, 2, \ldots, m-1 \end{cases} \quad (11)$$

According to Eq. (11), the shear complex stiffness at the outer boundary of the *j*th zone (viz. the inner boundary of the (*j* + 1)th zone) within the *i*th soil layer can be written as:

$$K_{i,j+1} = \frac{2\pi r_{i,j+1} G_{i,j}^{*} s_{i,j}\left[\dfrac{C_{i,j}}{D_{i,j}} \mathrm{K}_1\left(s_{i,j} r_{i,j+1}\right) \text{-} \mathrm{I}_1\left(s_{i,j} r_{i,j+1}\right)\right]}{\dfrac{C_{i,j}}{D_{i,j}} \mathrm{K}_0\left(s_{i,j} r_{i,j+1}\right) + \mathrm{I}_0\left(s_{i,j} r_{i,j+1}\right)} \quad (j = m-1, ..., 2, 1) \quad (12)$$

From Eq. (12) one obtains:

$$\frac{C_{i,j}}{D_{i,j}} = \frac{2\pi r_{i,j+1} G_{i,j}^{*} s_{i,j} \mathrm{I}_1\left(s_{i,j} r_{i,j+1}\right) + K_{i,j+1} \mathrm{I}_0\left(s_{i,j} r_{i,j+1}\right)}{2\pi r_{i,j+1} G_{i,j}^{*} s_{i,j} \mathrm{K}_1\left(s_{i,j} r_{i,j+1}\right) + K_{i,j+1} \mathrm{K}_0\left(s_{i,j} r_{i,j+1}\right)} \quad (13)$$

The recursion relation between $K_{i,j}$ and $K_{i,j+1}$ can be easily established by substituting Eq. (13) into Eq. (11), and then the vertical shear complex stiffness of pile-soil interface, $K_{i,1}$, can be obtained.

Solution of the Motion Equation of Pile

Denoting $\mathrm{U}_{\mathrm{p}i}(z,\xi) = \int_0^{\infty} u_{\mathrm{p}i}(z,t) e^{-\xi t} \mathrm{d}t$ to be the Laplace transform of $u_{\mathrm{p}i}(z,t)$ with respect to time *t*. Taking the Laplace transform of Eq. (2) and combining with the initial conditions Eq. (7) and Eq. (8) gives

$$v_{\mathrm{p}i}^{2}\left(1 + \frac{\delta_{\mathrm{p}i}\xi}{E_{\mathrm{p}i}} + \frac{\xi^2 \mu_{\mathrm{p}i}^{2} r_{\mathrm{p}i}^{2}}{v_{\mathrm{p}i}^{2}}\right)\frac{\partial^2 \mathrm{U}_{\mathrm{p}i}}{\partial z^2} - \left(\xi^2 + \frac{K_{i,1}}{\rho_{\mathrm{p}i} A_{\mathrm{p}i}}\right)\mathrm{U}_{\mathrm{p}i} = 0 \quad (14)$$

The general solution of Eq. (14) can be derived as

$$\mathrm{U}_{\mathrm{p}i} = M_i \cos(\frac{\overline{\lambda}_i z}{l_i}) + N_i \sin(\frac{\overline{\lambda}_i z}{l_i}) \quad (15)$$

where $\overline{\lambda}_i = \sqrt{-\left(\xi^2 + \frac{K_{i,1}}{\rho_{\mathrm{p}i} A_{\mathrm{p}i}}\right) t_i^2 / 1 + \frac{\delta_{\mathrm{p}i}\xi}{E_{\mathrm{p}i}} + \frac{\xi^2 \mu_{\mathrm{p}i}^2 r_{\mathrm{p}i}^2}{v_{\mathrm{p}i}^2}}$, is dimensionless eigenvalue; M_i and N_i are complex constants which can be derived according to the boundary conditions; $t_i = l_i / v_{\mathrm{p}i}$ denotes the propagation time of elastic longitudinal wave in the *i*th pile segment.

Combining the boundary conditions Eqs.(5) and (6), the displacement impedance function at the top of the *i*th pile segment can be given as

$$Z_{\mathrm{p}i}\Big|_{z=h_i} = -\frac{\rho_{\mathrm{p}i} A_{\mathrm{p}i} v_{\mathrm{p}i} (1 + \frac{\delta_{\mathrm{p}i}\xi}{E_{\mathrm{p}i}} + \frac{\xi^2 \mu_{\mathrm{p}i}^2 r_{\mathrm{p}i}^2}{v_{\mathrm{p}i}^2}) \overline{\lambda}_i \tan(\overline{\lambda}_i - \varphi_i)}{t_i} \quad (16)$$

where $\varphi_i = \arctan\left(Z_{\mathrm{p}i-1} t_i / \rho_{\mathrm{p}i} A_{\mathrm{p}i} v_{\mathrm{p}i} \overline{\lambda}_i \left(1 + \frac{\delta_{\mathrm{p}i}\xi}{E_{\mathrm{p}i}} + \frac{\xi^2 \mu_{\mathrm{p}i}^2 r_{\mathrm{p}i}^2}{v_{\mathrm{p}i}^2} \right) \right)$, $Z_{\mathrm{p}i-1}$ is the displacement impedance function at the top of the (*i*-1)th pile segment which can be obtained by the boundary conditions.

Then, based on the impedance function transfer method, the displacement impedance function at the pile head can be derived as

$$Z_{\mathrm{p}n}\Big|_{z=h_n=0} = -\frac{\rho_{\mathrm{p}n} A_{\mathrm{p}n} v_{\mathrm{p}n} (1 + \frac{\delta_{\mathrm{p}n}\xi}{E_{\mathrm{p}n}} + \frac{\xi^2 \mu_{\mathrm{p}n}^2 r_{\mathrm{p}n}^2}{v_{\mathrm{p}n}^2}) \overline{\lambda}_n \tan(\overline{\lambda}_n - \varphi_n)}{t_n} \quad (17)$$

where $\varphi_n = \arctan\left(Z_{\mathrm{p}n-1} t_n / \rho_{\mathrm{p}n} A_{\mathrm{p}n} v_{\mathrm{p}n} \overline{\lambda}_n \left(1 + \frac{\delta_{\mathrm{p}n}\xi}{E_{\mathrm{p}n}} + \frac{\xi^2 \mu_{\mathrm{p}n}^2 r_{\mathrm{p}n}^2}{v_{\mathrm{p}n}^2} \right) \right)$.

$Z_{\mathrm{p}n}$ can be further rewritten as

$$Z_{\mathrm{p}n} = \mathrm{Re}(Z_{\mathrm{p}n}) + \mathrm{j} \cdot \mathrm{Im}(Z_{\mathrm{p}n}) \quad (18)$$

where $\mathrm{Re}(Z_{pn})$ and $\mathrm{Im}(Z_{pn})$ are dynamic stiffness and dynamic damping which reflect the ability of pile-soil system to resist vertical deformation and vertical vibration, respectively.

PARAMETRIC STUDY AND DISCUSSION

In this section, a parametric study is conducted to investigate the vertical dynamic impedance of large-diameter pile based on the solution in Eq. (18). First, the influence of the number of soil zone is discussed. Then, the influence of the transverse inertia effect on the dynamic impedance at pile head for different pile-soil parameters is investigated in detail.

Influence of the Number of the Soil Zone

In order to simulate the radial inhomogeneity of the surrounding soil caused by the construction disturbance effect, the shear complex stiffness transfer model is presented in this paper in which the surrounding soil is divided into finite annular zones. As a result, it is necessary to investigate the influence of the number of the soil zone on the calculated results. In the following analysis, the length, radius, dynamic Poisson ratio, elastic longitudinal wave velocity, material damping and density of pile are $l_p = 10\mathrm{m}$, $r_p = 0.5\mathrm{m}$, $\mu_p = 0.2$, $v_p = 3600\mathrm{m/s}$, $\delta_p = 100000\mathrm{N \cdot s/m^2}$ and $\rho_p = 2500\mathrm{kg/m^3}$, respectively. The density and dynamic Poisson ratio of the pile end soil and the surrounding soil are $1800\mathrm{kg/m^3}$ and 0.4, respectively. The width of the disturbed zone is $r_b = 1r_p$. The shear wave velocity of the pile end soil is $150\mathrm{m/s}$, while that of the surrounding soil from the outer undisturbed zone to the inner disturbed zone decreases linearly from $150\mathrm{m/s}$ to $100\mathrm{m/s}$. The number of the soil zone are set to be m = 2, 5, 10, 20 and 30, respectively.

The influence of the number of the soil zone on the dynamic impedance at the pile head is shown in **Figure 2**, where f represents the frequency. It can be seen that as the number of the soil zone increases, both the dynamic stiffness and the dynamic damping tend to be convergent. When the number of the soil zone is big enough, namely $m \geq 20$ in this case, the computational curves will coincide completely. Therefore, the number of the soil zone is set to be twenty in the following analysis.

Relationship between the Transverse Inertia Effect and the Pile Parameters

Radius of Pile

Parameters used in this section are given as follows: the pile radius are $r_{\mathrm{p}} = 0.3\mathrm{m}$, $0.5\mathrm{m}$ and $0.7\mathrm{m}$, respectively; dynamic Poisson ratio of the pile are $\mu_{\mathrm{p}} = 0$ and 0.2, respectively, where $\mu_{\mathrm{p}} = 0$ means that the transverse inertia effect of the pile is not considered. Other parameters are the same as shown in section 4.1.

Figure 3 shows the influence of the transverse inertia effect on the dynamic impedance at the pile head with different pile radius. It is evident that with the increase of the radius of pile, the oscillation amplitude of the dynamic stiffness and the dynamic damping increases. It can also be noted that when the transverse inertia effect is considered, the resonant frequencies and oscillation amplitude of the dynamic impedance decrease and the decrease rate increases with the increase of frequency and pile radius.

Dynamic Poisson Ratio of Pile

The transverse inertia effect is directly related to the dynamic Poisson ratio of pile. Therefore, it is necessary to analyze the influence of the dynamic Poisson ratio of pile on the dynamic impedance at the pile head. In this section, the dynamic Poisson ratio of pile are $\mu_{\mathrm{p}} = 0$, 0.15, 0.2 and 0.25, respectively.

The influence of the dynamic Poisson ratio of pile on the dynamic impedance at the pile head is shown in **Figure 4**. It can be noted that when the frequency is less than $450\mathrm{Hz}$, the dynamic Poisson ratio has little influence on the dynamic impedance at the pile head. While within the higher frequency range (more than $450\mathrm{Hz}$ in this case), the decreasing trend of the resonant frequencies of the dynamic impedance becomes more notable with the increase of frequency and the dynamic Poisson ratio of pile.

Influence of the Construction Disturbance Effect

During pile construction, the surrounding soil may be strengthened or weakened, making the soil inhomogeneous radially. In this section, the influence of the construction disturbance effect on the dynamic impedance at the pile head as well as its relationship with the transverse inertia effect is investigated.

Influence of the Disturbance Range

First, the influence of the hardening range of pile surrounding soil on the dynamic impedance is analyzed. Parameters adopted here are as follows: the shear wave velocity of the surrounding soil from the outer undisturbed zone to inner disturbed zone increases linearly from 150m/s to 200m/s; the width of the disturbed zone are $r_b = 0r_p$, $1r_p$ and $2r_p$, respectively, where $r_b = 0r_p$ means that the surrounding soil is homogeneous in the radial direction. Other parameters are the same as shown in section 4.1.

The influence of the hardening range changing within larger scale on the dynamic impedance at the pile head is shown in **Figure 5**. It can be observed that compared with the result for the radially homogeneous case, the oscillation amplitude of the dynamic impedance decreases significantly and the decrease of the resonant frequencies of the dynamic impedance when considering the transverse inertia effect has a slight decrease for the radially hardening case. Further increase of the hardening range has little influence on the dynamic impedance when it reaches the value of $1r_p$, which means that the soil adjacent to the pile has more significant influence on the dynamic characteristic of pile than that of the far-field.

In order to investigate the influence of the hardening range on the dynamic impedance at the pile head in more detail, the influence of the hardening range changing within smaller scale is analyzed. In the following analysis, the width of the hardening range are $r_b = 0r_p$, $0.05r_p$, and $0.1r_p$, respectively.

Figure 6 shows the influence of the hardening range changing within smaller scale on the dynamic impedance at the pile head. It is evident that the decrease of the oscillation amplitude of the dynamic impedance tends to be convergent with the increase of the hardening range, which indicates that the hardening effect still has a significant influence on the dynamic impedance at the pile head even if the surrounding soil is hardened within a small scale. Besides, the influence of the transverse inertia effect on the dynamic impedance at the pile head decreases slightly as the hardening range of the surrounding soil increases within smaller scale.

Then, the influence of the softening range of the surrounding soil on the dynamic impedance at the pile head is discussed. Parameters used here are given as follows: the shear wave velocity of the surrounding soil from the outer undisturbed zone to inner disturbed zone decreases linearly from 150m/s to 100m/s; the width of the softening range are $r_b = 0r_p$, $1r_p$ and $2r_p$, respectively.

Figure 7 shows the influence of the softening range changing within larger scale on the dynamic impedance at the pile head. It can be noted that the oscillation amplitude of the dynamic impedance for the radially softening soil increases significantly compared with the result for the radially homogeneous case. The dynamic impedance corresponding to a softening range of $1r_{\mathrm{p}}$ coincides completely with that corresponding to a softening range of $2r_{\mathrm{p}}$, demonstrating, once again, that it is the soil adjacent to the pile that greatly affects the dynamic characteristic of the pile rather than that of the far-field. **Figure 7** also shows that when the transverse inertia effect is considered, the decrease of the resonant frequencies of the dynamic impedance increases slightly for the radially softening soil compared with the radially homogeneous case.

Likewise, the influence of the softening range within smaller scale on the dynamic impedance at the pile head is studied and the result is shown in **Figure 8**. It can be noted that the oscillation amplitude of the dynamic impedance increases as the softening range increases but the increase rate decreases, which means that, even if the construction disturbance effect softens the surrounding soil within smaller scale, it also has a notable influence on the dynamic impedance at the pile head. It can also be seen from **Figure 8** that the influence of the transverse inertia effect is slightly greater for higher softening range.

Influence of Disturbance Degree

Firstly, the influence of the hardening degree of the surrounding soil on the dynamic impedance at the pile head is investigated. Parameters used here are given as follows: the width of the disturbed zone is $r_{\mathrm{b}} = 1r_{\mathrm{p}}$; shear wave velocity of the outer undisturbed zone is $150\mathrm{m/s}$; the shear wave velocity of the surrounding soil increases linearly radially inwards from $150\mathrm{m/s}$ to $200\mathrm{m/s}$, $250\mathrm{m/s}$ and $300\mathrm{m/s}$, respectively, which correspond to three cases (viz case *A*, *B* and *C*, respectively) that the strengthening degree of the soil increases.

The influence of the hardening degree on the dynamic impedance at the pile head is shown in **Figure 9**. It can be noted that the oscillation amplitude of the dynamic impedance decreases with the increase of the hardening degree of the soil, but the decrease rate decreases gradually. It should be pointed out that when considering the transverse inertia effect, the decreasing trend of the resonant frequencies of the dynamic impedance becomes less notable as the hardening degree increases.

Then, the influence of the softening degree is studied. In this section, the shear wave velocity of the surrounding soil decreases radially inwards from $150\mathrm{m/s}$ to $120\mathrm{m/s}$, $90\mathrm{m/s}$

and 60m/s respectively, which correspond to three cases (viz case *a*, *b* and *c*, respectively) that the softening degree of the soil increases.

Figure 10 shows the influence of the softening degree on the dynamic impedance at the pile head. It can be observed that, with the increase of the softening degree, the oscillation amplitude of the dynamic impedance increases, and the decrease of the resonant frequencies of the dynamic impedance has a slight increase when the transverse inertia effect is considered.

COMPARISON WITH OTHER SOLUTIONS

The present solution can be degenerated into the solution that does not consider the transverse inertia effect of pile when the dynamic Poisson ratio of pile is set to be zero. On this basis, comparisons are conducted with two other published solutions to verify the reliability of the present solution.

The comparison of the proposed solution for an end bearing pile with that of Yang and Tang (2013) is shown in **Figure 11**, where $\kappa = \mathrm{Re}(Z_{\mathrm{p}n}) / \lim_{\omega \to 0} \mathrm{Re}(Z_{\mathrm{p}n})$, $\eta = \mathrm{Im}(Z_{\mathrm{p}n}) / \varpi$ and $\varpi = r_{\mathrm{p}} \omega / v_{\mathrm{s}}$ represent non-dimensional dynamic stiffness, non-dimensional dynamic damping and non-dimensional circular frequency adopted in reference (Yang and Tang 2013), respectively. The solution of Yang and Tang (2013) is the special case of the present solution without considering the radial inhomogeneity. It is evident that the dynamic stiffness and damping for the present solution are in basically agreement with those for the solution of Yang and Tang (2013), respectively. It can also be seen that compared with the degenerate solution, the resonant frequencies of both dynamic stiffness and damping decrease for the present solution as well as the solution of Yang and Tang (2013), demonstrating a significant influence of transverse inertia effect on the dynamic impedance of large-diameter pile.

The comparison of the proposed solution with that of Yang et al. (2009) which did not consider the transverse inertia effect is shown in **Figure 12**. It can be obtained that the dynamic stiffness and damping for the degenerate solution and the solution of Yang et al. (2009) are consistent, respectively, and the resonant frequencies of both of which decrease slightly when the transverse inertia effect is considered. It is worth noting that, because of a much bigger length-diameter ratio, the influence of transverse inertia effect is much weaker than that shown in **Figure 11**.

As the complicated geological conditions in the marine and coastal areas, there may exist some errors between the calculated results and the actual engineering. Even so, the present solution can also provide a reference for the dynamic design of large-diameter pile.

CONCLUSIONS

By utilizing the shear complex stiffness transfer model to simulate the radial inhomogeneity of soil, and the Rayleigh-Love rod model to consider the transverse inertia effect of pile, the analytical solution of vertical dynamic impedance at the head of the large-diameter pile is obtained. A comprehensive parametric study is presented and the results show that both the transverse inertia effect and the construction disturbance effect have significant influence on the dynamic impedance at the pile head.

(1) When the transverse inertia effect is considered, the resonant frequencies of both the dynamic stiffness and damping at the pile head decrease at high frequencies, and the reduction in the resonant frequencies increases with the increase of frequency, pile radius and the dynamic Poisson ratio of pile.

(2) The construction disturbance effect of the pile surrounding soil has its range of influence on the dynamic impedance at the pile head. Within this range, the oscillation amplitude of the dynamic impedance at the pile head decreases with the increase of hardening range and hardening degree, while increases as the softening range and softening degree increase; the influence of the transverse inertia effect on the dynamic impedance at the pile head has a slight decrease with the increase of the hardening range and hardening degree, while increases slightly as the softening range and softening degree increase.

(3) The influence of the transverse inertia effect on the dynamic impedance at the pile head increases significantly with the increase of the radius and dynamic Poisson ratio of pile, which is, in relative terms, less sensitive to the construction disturbance effect, demonstrating that the influence of the transverse inertia effect on the dynamic impedance at the pile head is more affected by the pile parameters than by the soil parameters.

(4) It is shown by comparing with the solutions of Yang and Tang (2013) and Yang et al. (2009) that the present solution has sufficient accuracy.

Acknowledgements

This research is supported by the National Natural Science Foundation of China (Grant No. 51378464 and No. 51579217).

References

Chai, H. Y., K. K. Phoon, and D. J. Zhang. 2010. Effects of the source on wave propagation in pile integrity testing. *Journal of Geotechnical and Geoenvironmental Engineering* 136 (9):1200–08. doi:10.1061/(asce)gt.1943-5606.0000272

Chai, H. Y., C. F. Wei, K. K. Phoon, and Y. M. Yang. 2011. Some observations on the performance of the signal matching technique in assessment of pile integrity. *Journal of Nondestructive Evaluation* 30:246–58. doi:10.1007/s10921-011-0113-9

Chow, Y. K., K. K. Phoon, W. F. Chow, and K. Y. Wong. 2003. Low strain integrity testing of piles: Three-dimensional effects. *Journal of Geotechnical and Geoenvironmental Engineering* 129 (11):1057–62. doi:10.1061/(asce)1090-0241(2003)129:11(1057)

El Naggar, M. H. 2000. Vertical and torsional soil reactions for radially inhomogeneous soil layer. *Structural Engineering and Mechanics* 10 (4):299–312. doi:10.12989/sem.2000.10.4.299

El Naggar, M. H., and J. Q. Wei. 2000. Uplift behaviour of tapered piles established from model tests. *Canadian Geotechnical Journal* 37 (1):56–74. doi:10.1139/t99-090

Gao, G. Y., C. B. Yang, M. Gao, and J. Zhang. 2012. Influence of bearing stratum on vertical bearing behaviors of large diameter cast-in-place belled piles. *Chinese Journal of Geotechnical Engineering* 34 (7):1184–91. (in Chinese)

Gao, M., G. Y. Gao, B. H. Gu, and C. B. Yang. 2012. Practical method for settlement calculation of large-diameter belled piles. *Chinese Journal of Geotechnical Engineering* 34 (8):1448–52. (in Chinese)

Gong, C. Z., C. L. He, W. M. Gong, and G. L. Dai. 2012. Analysis of size effect on large diameter rock-socketed pile based on self-balance method. *Rock and Soil Mechanics* 33 (8):2403–07.

Han, Y. C., and G. C. W. Sabin. 1995. Impedances for radially inhomogeneous viscoelastic soil media. *Journal of Engineering Mechanics Division* 121 (9):939–47. doi:10.1061/(asce)0733-9399(1995)121:9(939)

He, C. L, C. Z. Gong, F. Gong, and Y. Hu. 2015. Laboratory test on the effect of diameter and depth of rock-socketed Piles. *Chinese Journal of Underground Space and Engineering* 11 (2):293–98.

Kodikara, J. K., and I. D. Moore. 1993. Axial response of tapered piles in cohesive frictional ground. *Journal of Geotechnical Engineering* 119 (4):675–93. doi:10.1061/(asce)0733-9410(1993)119:4(675)

Li, Q., K. H. Wang, and K. H. Xie. 2005. Dynamic response for vertical vibration of large diameter pile in saturated soil. *Journal of Vibration Engineering* 18 (4):500–05. (in Chinese)

Li, Z. G., and Y. L. Gong. 1998. Discussion on three dimensional effect of wave propagating in the pile with large diameter. *Chinese Journal of Rock Mechanics and Engineering* 17 (4):434–39. (in Chinese)

Liu, F. T., C. F. Zhao, J. Wu, and D. Liu. 2010. Experimental research on bearing behavior and size effect of large diameter bored cast-in-situ piles in Changzhou area. *Chinese Journal of Rock Mechanics and Engineering* 29 (4):858–64.

Liu, X. R., T. Fang, D. X. Geng, Z. J. Wu, and X. T. Ji. 2013. Model test on lateral bearing behaviors of large diameter pile with variable cross section. *China Journal of Highway and Transport* 26 (6):80–86. (in Chinese)

Lü, S. H., K. H. Wang, W. B. Wu, and C. H. Leo. 2014. Longitudinal vibration of a pile embedded in layered soil considering the transverse inertia effect of pile. *Computers and Geotechnics* 62:90–99. doi:10.1016/j.compgeo.2014.06.015

Novak, M. 1974. Dynamic stiffness and damping of piles. *Canadian Geotechnical Journal* 11 (4):574–98. doi:10.1139/t74-059

Novak, M., F. Aboul-Ella, and T. Nogami. 1978. Dynamic soil reactions for plane strain case. *Journal of the Engineering Mechanics Division* 104 (4):953–59.

Novak, M., and Han, Y. C. 1988. Impedances of soil layer with disturbed boundary zone. *Journal of the Geotechnical Engineering* 114 (9):1002–21.

Novak, M., and M. Sheta. 1980. Approximate approach to contact problems of piles. Proceedings of the Geotechnical Engineering Division. National Convention, Florida, 53–79.

Pells, P. J. N., R. K. Rowe, and R. M. Turner. 1980. An experimental investigation into side shear for socketed piles in sandstone. Proceedings of the International Conference on Structural Foundations on Rock, Sydney: [s. n.] 1, 291–302.

Randolph, M. F., and A. J. Deeks. 1992. Dynamic and static soil models for axial pile response. Proceedings of the 4th International Conference on the Application of Stress Wave Theory to Piles, The Hague, The Netherlands, 21–24.

Veletos, A. S., and K. W. Dotson. 1986. Impedances of soil layer with disturbed boundary zone. *Journal of the Geotechnical Engineering* 112 (3):363–68. doi:10.1061/(asce)0733-9410(1986)112:3(363)

Veletos, A. S., and K. W. Dotson. 1988. Vertical and torsional vibration of foundations in inhomogeneous media. *Journal of the Geotechnical Engineering* 114 (9):1002–21.

Wu, W. B., K. H. Wang, and B. Dou. 2013. Vertical dynamic response of a viscoelastic tapered pile embedded in layered foundation. *Journal of Vibration and Shock* 32 (8):120–27. (in Chinese)

Wu, W. B., K. H. Wang, Z. Q. Zhang, and C. J. Leo. 2013. Soil-pile interaction in the pile vertical vibration considering true three-dimensional wave effect of soil. *International Journal for Numerical and Analytical Methods in Geomechanics* 37 (17):2860–76.

Yang, D. Y., K. H. Wang, Z. Q. Zhang, and C. J. Leo. 2009. Vertical dynamic response of pile in a radially heterogeneous soil layer. *International Journal for Numerical and Analytical Methods in Geomechanics* 33 (8):1039–54. doi:10.1002/nag.755

Yang, X., and J. Tang. 2013. Vertical vibration of single pile with transversal inertia effect in stratified saturated soil. *Rock and Soil Mechanics* 34 (6):1560–66. (in Chinese)

Yu, J., Y. Y. Cai, and W. B. Wu. 2013. Effect of sediment on vertical dynamic impedance of rock-socketed pile with large diameter. *Journal of Central South University* 20 (10):2856–62. doi:10.1007/s11771-013-1806-2

Zhang, J. X., D. Y. Wu, and S. C. Zhang. 2007. Finite element analysis of size effect of rock-socketed piles. *Rock and Soil Mechanics* 28 (6):1221–24.

Zhao, C. F., J. Li, Z. X. Qiu, C. Zhao, and Y. W. Zou. 2015. Experimental research on load transfer of large-diameter and super-long bored pile in Guangdong area. *Chinese Journal of Rock Mechanics and Engineering* 34 (4):849–55. (in Chinese)

Zhu, B., Y. Y. Yang, Z. G. Yu, J. F. Guo, and Y. M. Chen. 2012. Filed tests on lateral monotonic and cyclic loadings of offshore elevated piles. *Chinese Journal of Geotechnical Engineering* 34 (6):1028–37. (in Chinese)

Figure 1. Schematic diagram of the soil-pile interaction model

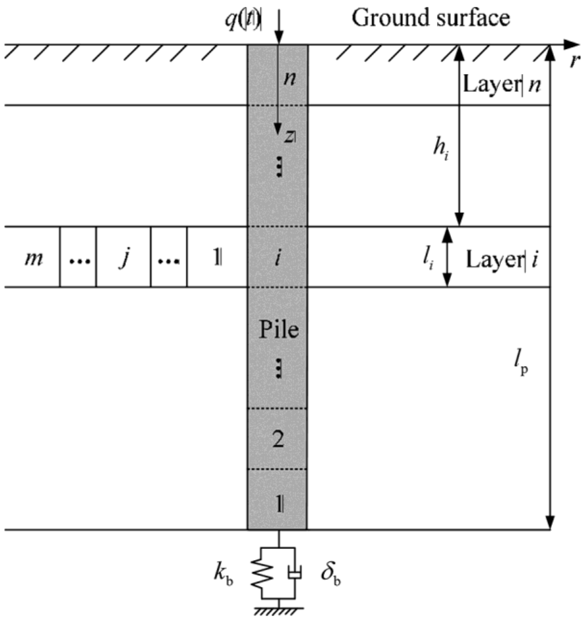

Figure 2. Influence of the number of the soil zone on the dynamic impedance at the pile head; (a) Dynamic stiffness; (b) Dynamic damping

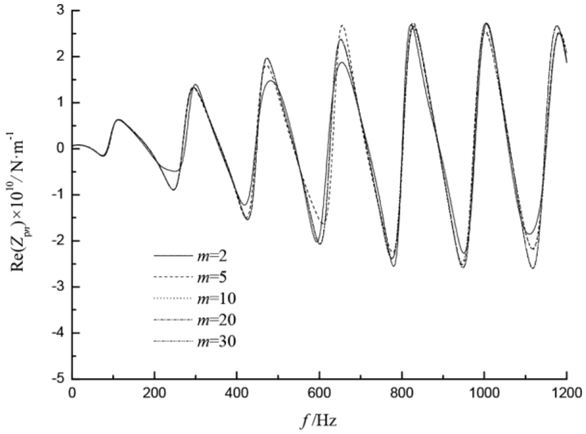

(a) Dynamic stiffness

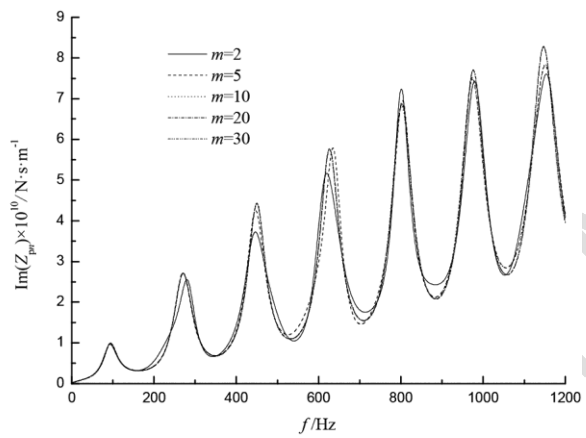

(b) Dynamic damping

Figure 3. Influence of the transverse inertia effect on the dynamic impedance at the pile head with different pile radius; (a) Dynamic stiffness; (b) Dynamic damping

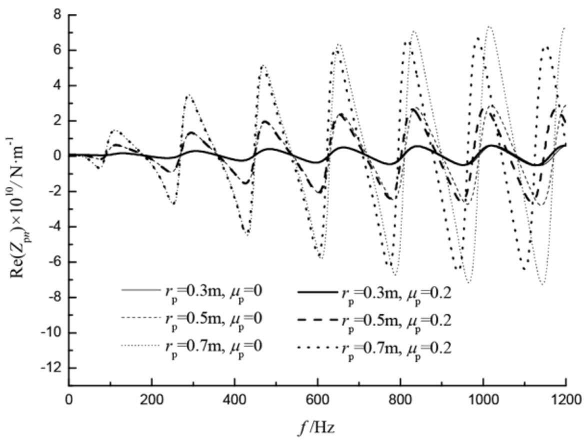

(a) Dynamic stiffness

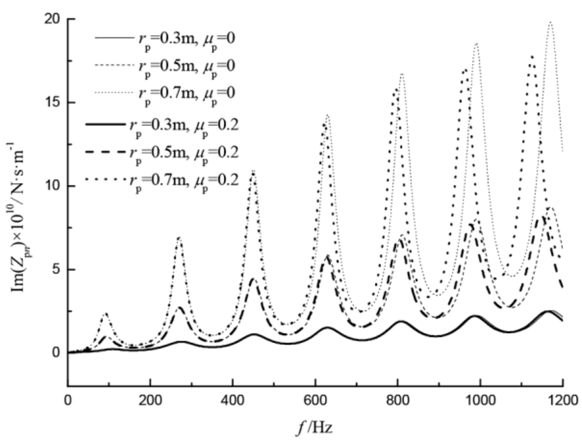

(b) Dynamic damping

Figure 4. Influence of the dynamic Poisson ratio of pile on the dynamic impedance at the pile head; (a) Dynamic stiffness; (b) Dynamic damping

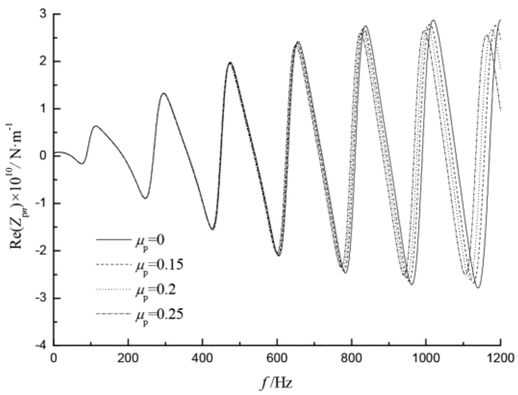

(a) Dynamic stiffness

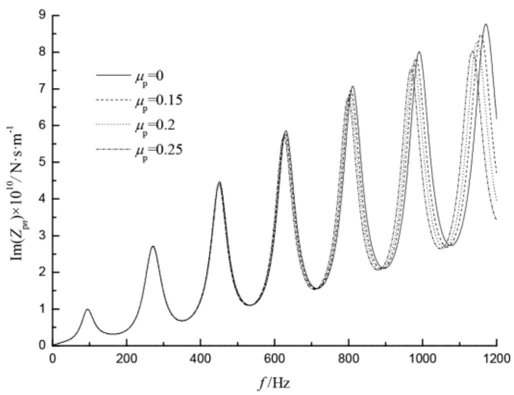

(b) Dynamic damping

Figure 5. Influence of the hardening range changing within larger scale on the dynamic impedance at the pile head; (a) Dynamic stiffness; (b) Dynamic damping

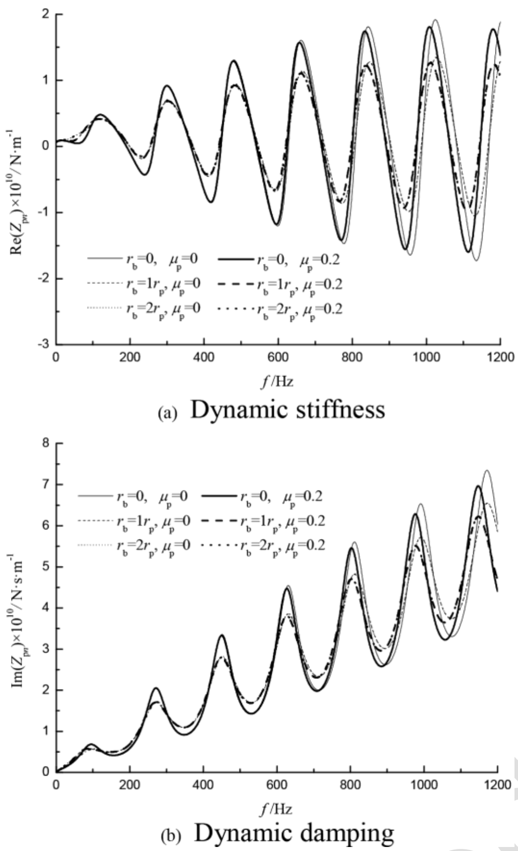

Figure 6. Influence of the hardening range changing within smaller scale on the dynamic impedance at the pile head; (a) Dynamic stiffness; (b) Dynamic damping

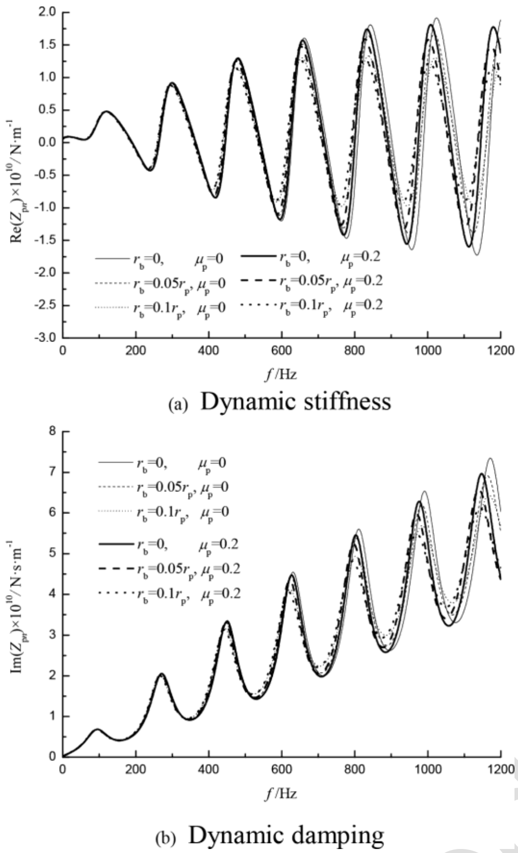

Figure 7. Influence of the softening range changing within larger scale on the dynamic impedance at the pile head; (a) Dynamic stiffness; (b) Dynamic damping

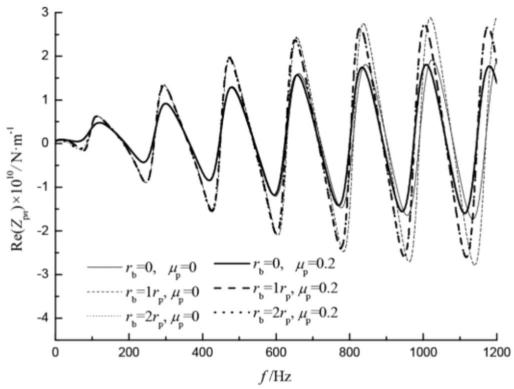

(a) Dynamic stiffness

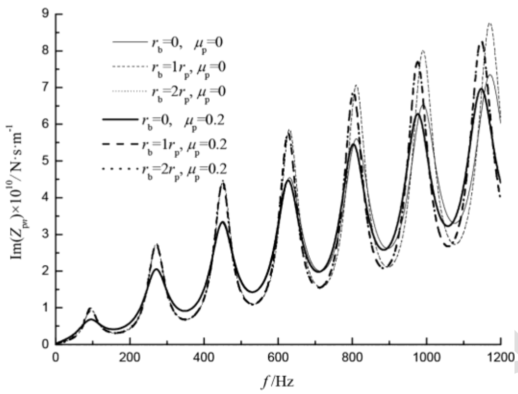

(b) Dynamic damping

Figure 8. Influence of the softening range changing within smaller scale on the dynamic impedance at the pile head; (a) Dynamic stiffness; (b) Dynamic damping

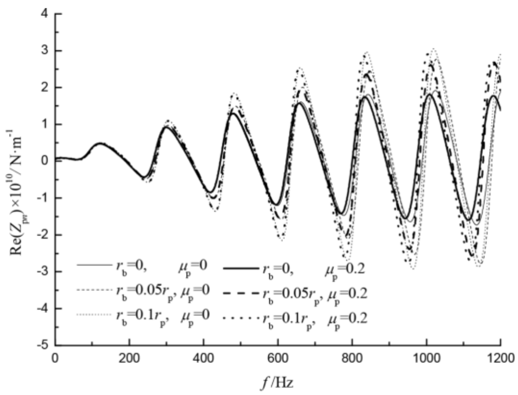

(a) Dynamic stiffness

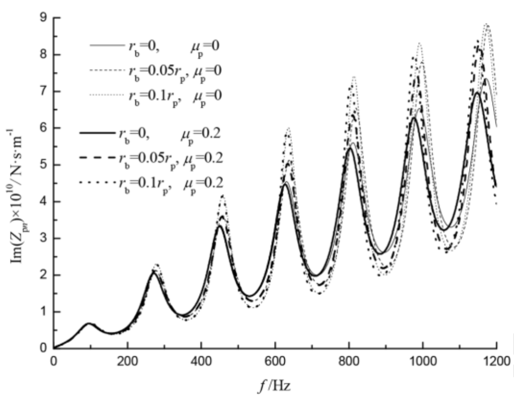

(b) Dynamic damping

Figure 9. Influence of the hardening degree on the dynamic impedance at the pile head; (a) Dynamic stiffness; (b) Dynamic damping

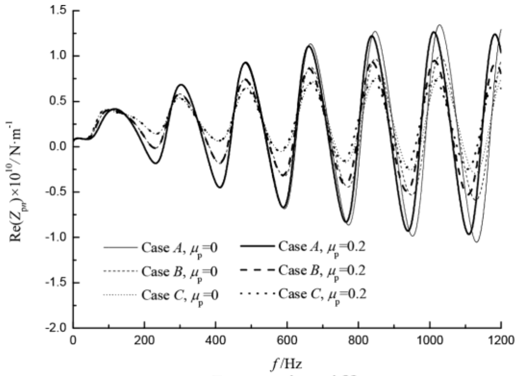

(a) Dynamic stiffness

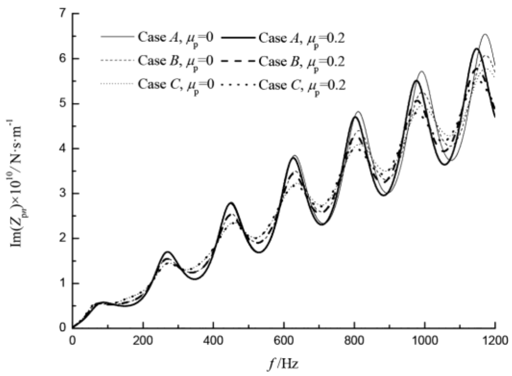

(b) Dynamic damping

Figure 10. Influence of the softening degree on the dynamic impedance at the pile head; (a) Dynamic stiffness; (b) Dynamic damping

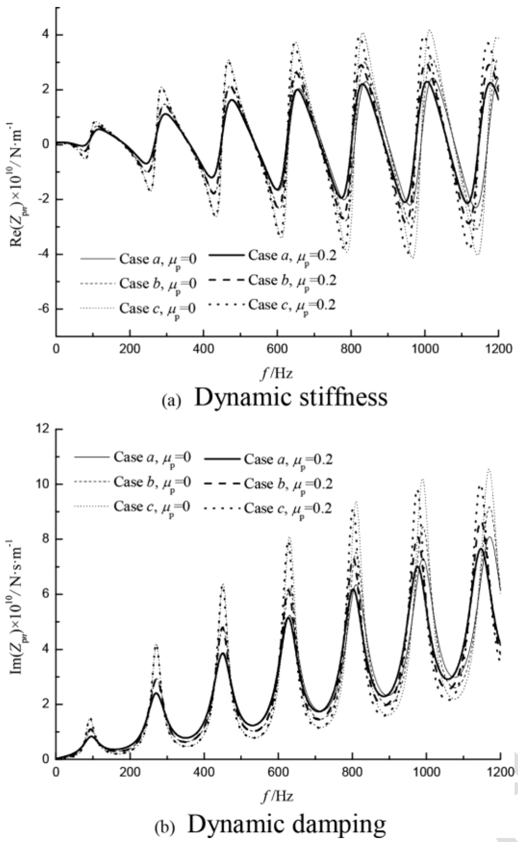

Figure 11. Comparison of dynamic impedance with the solution of Yang and Tang (2013); (a) Dynamic stiffness; (b) Dynamic damping

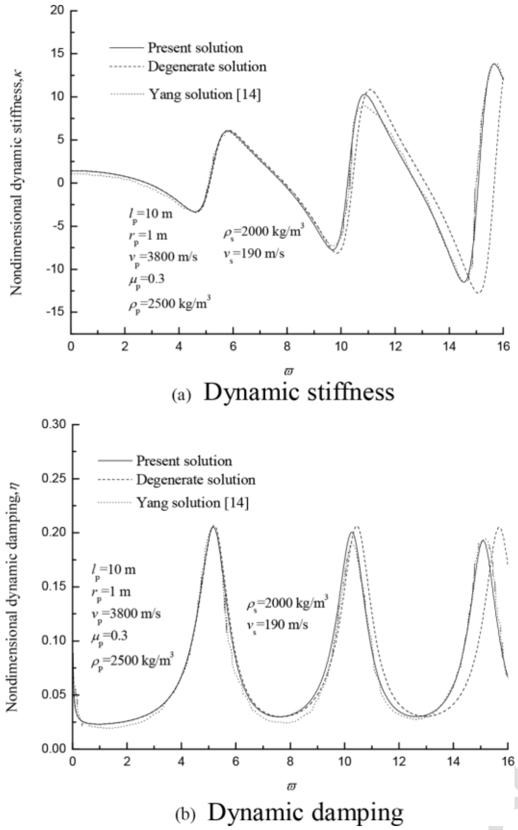

Figure 12. Comparison of dynamic impedance with the solution of Yang et al. (2009); (a) Dynamic stiffness; (b) Dynamic damping

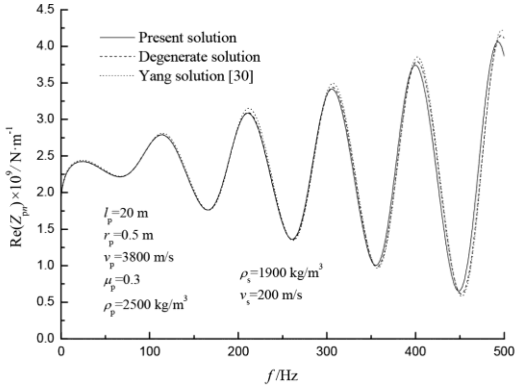

(a) Dynamic stiffness

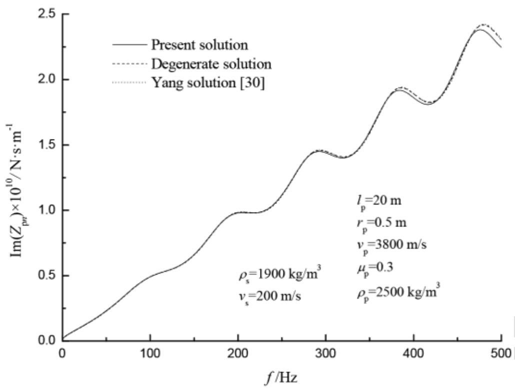

(b) Dynamic damping